TU Delft

Delft University of Technology

Framework for Simultaneous Sensor and Actuator Fault-Tolerant Flight Control

Lu, Peng; van Kampen, Erik-Jan; de Visser, Coen; Chu, Qiping

DOI
10.2514/1.G002079

Publication date
2017

Document Version
Accepted author manuscript

Published in
Journal of Guidance, Control, and Dynamics: devoted to the technology of dynamics and control

Citation (APA)
Lu, P., van Kampen, E.-J., de Visser, C., & Chu, Q. (2017). Framework for Simultaneous Sensor and Actuator Fault-Tolerant Flight Control. *Journal of Guidance, Control, and Dynamics: devoted to the technology of dynamics and control*. https://doi.org/10.2514/1.G002079

Important note
To cite this publication, please use the final published version (if applicable).
Please check the document version above.

Copyright
Other than for strictly personal use, it is not permitted to download, forward or distribute the text or part of it, without the consent of the author(s) and/or copyright holder(s), unless the work is under an open content license such as Creative Commons.

Takedown policy
Please contact us and provide details if you believe this document breaches copyrights.
We will remove access to the work immediately and investigate your claim.

This work is downloaded from Delft University of Technology.
For technical reasons the number of authors shown on this cover page is limited to a maximum of 10.

This is an Accepted Manuscript of an article published in: Journal of Guidance, Control, and Dynamics
Vol. 40, No. 8 (2017), pp. 2133-2136
Available online: https://doi.org/10.2514/1.G002079

A Framework for Simultaneous Sensor and Actuator Fault-Tolerant Flight Control

P. Lu[1], E. van Kampen[2], C.C. de Visser[3], Q.P. Chu[4]
Delft University of Technology, P.O. Box 5058, 2600 GB Delft, The Netherlands

I. Introduction

In civil aviation, many developments focus on improving the safety levels and reducing the risks that critical faults occur [1]. According to [2], loss of control in-flight is one of the three high-risk accident categories. Some recent accidents caused by actuator faults include [3] and [4]. To avoid these accidents, the flight control systems should be reconfigurable in the presence of actuator faults. This motivates the development of actuator Fault-Tolerant Control (FTC) systems.

Apart from actuator faults, recent airliner accidents indicate that sensor faults can result in critical failures [5]. Some recent accidents caused by sensor failures include [6] and [7]. These examples highlight the importance of sensor Fault Detection and Diagnosis (FDD) systems. In the past few decades, many promising sensor FDD approaches have been proposed [8–13].

Most sensor FDD approaches use the aircraft aerodynamic model, which calculates the aerodynamic forces and moments. Furthermore, these FDD approaches are usually designed based on linear time invariant systems [14]. The aerodynamic forces and moments acting on the aircraft can change significantly under different flight conditions. To reduce the influence of nonlinearities during the whole flight, a Linear Parameter Varying (LPV) system, which may explicitly contain information about the aerodynamic coefficient variations over the flight envelope [15], can be designed. However, the modeling of this LPV system can be time-consuming. Alternatively, the aircraft kinematic model [12, 13, 16–18], which does not require the modeling of an LPV system,

[1] Ph.D. Student, Control and Simulation Division; P.Lu-1@tudelft.nl.
[2] Assistant Professor, Control and Simulation Division; e.vankampen@tudelft.nl
[3] Assistant Professor, Control and Simulation Division; c.c.devisser@tudelft.nl
[4] Associate Professor, Control and Simulation Division; q.p.chu@tudelft.nl

can be applied. The core of the kinematic model is that it uses measured specific forces to reduce model uncertainties. This model has been used for sensor FDD and shows great potentials.

The fault information provided by FDD systems can be used to compensate the influence of sensor faults. To deal with actuator faults, a reconfigurable controller is required [19]. Various reconfigurable controllers are proposed for aerospace applications [8, 19–22]. [23] uses model predictive control which can handle system input and output constraints. Sliding mode control [24] is also applied to FTC due to its fast convergence property [24]. H_∞ control approach has also been proposed to design FTC controllers [25]. Additionally, Backstepping (BS) is one of the popular Lyapunov-based control approaches which can be used for designing FTC systems. However, standard BS is sensitive to model uncertainties. To cope with model uncertainties, Adaptive Backstepping [26] and Command Filtering Backstepping [27] were proposed. More recently, Incremental Backstepping (IBS) [28, 29], which can cope with model uncertainties, is proposed.

Although several sensor FDD systems and actuator FTC systems are proposed [19, 30, 31], research on simultaneous sensor and actuator FTC system is limited. One reason is that state-of-the-art sensor FDD systems make use of actuator information such as commanded control surface deflections. It can lead to incorrect sensor FDD when the actuator fails resulting in wrong information from the actuator. Recently, Zhang and li [32], Marzat et. al [33] and Alwi et. al [14] consider simultaneous sensor and actuator FDD. However, simultaneous sensor and actuator FTC is not dealt with. Furthermore, performance of existing sensor FDD systems is only shown in off-line simulation. In this paper, simultaneous sensor and actuator FTC is considered and the performance is shown in online simulation. To the best of the authors' knowledge, the present paper is one of the first papers which consider simultaneous aircraft sensor and actuator FTC.

The present paper aims at proposing a framework of FTC systems which is able to deal with simultaneous sensor and actuator faults. The FTC system is composed of a sensor FDD system and a reconfigurable controller. The sensor FDD system is designed by making use of an aircraft kinematic model which does not require actuator deflections. The detection and estimation of the sensor faults are resolved using an Adaptive Three-Step Unscented Kalman Filter (ATS-UKF) [13] which can estimate the state and fault in an unbiased sense. The unbiased state estimation is

provided to the reconfigurable controller such that FTC in the presence of sensor faults is achieved. Regarding actuator and process faults, the IBS approach is applied to reconfigure the controller. By doing this, simultaneous sensor and actuator FTC is achieved. It should be noted that [13] only validates sensor FDD in off-line simulation while the validation in this paper is online. In addition, [13] does not consider Aircraft Heading and Reference System (AHRS) faults and actuator faults.

The performance of the proposed FTC system is validated. The control objective is to control the aircraft attitude. An attitude controller and an angular rate controller are designed based on the IBS approach. Command filters are implemented to take the actuator physical limits into consideration. The aircraft sensor faults contain Air Data Sensors (ADS) and AHRS faults. Aileron and rudder faults are considered. The FTC system is applied to address the sensor and actuator FTC simultaneously and maintain controlled flight.

II. Sensor Fault Reconstruction System Design

In this section, first the model used for sensor fault reconstruction is introduced in section II A. Then the detailed sensor fault reconstruction system design is presented in section II B.

A. Nonlinear aircraft kinematic model including ADS and AHRS faults

The model used for sensor fault reconstruction is the aircraft kinematic model. It should be noted that this model does not require any information of the actuator. The process model including

ADS and AHRS faults is presented as follows [13]:

$$\dot{V} = (A_{xm} - w_{Ax} - g\sin\theta)\cos\alpha\cos\beta + (A_{ym} - w_{Ay} + g\sin\phi\cos\theta)\sin\beta$$
$$+ (A_{zm} - w_{Az} + g\cos\phi\cos\theta)\sin\alpha\cos\beta \tag{1}$$

$$\dot{\alpha} = \frac{1}{V\cos\beta}\big[-(A_{xm} - w_{Ax})\sin\alpha + (A_{zm} - w_{Az})\cos\alpha + g\cos\phi\cos\theta\cos\alpha$$
$$+ g\sin\theta\sin\alpha\big] + q_m - w_q - [(p_m - w_p)\cos\alpha + (r_m - w_r)\sin\alpha]\tan\beta \tag{2}$$

$$\dot{\beta} = \frac{1}{V}\big[-(A_{xm} - w_{Ax} - g\sin\theta)\cos\alpha\sin\beta + (A_{ym} - w_{Ay} + g\sin\phi\cos\theta)\cos\beta$$
$$-(A_{zm} - w_{Az} + g\cos\phi\cos\theta)\sin\alpha\sin\beta\big] + (p_m - w_p)\sin\alpha - (r_m - w_r)\cos\alpha \tag{3}$$

$$\dot{\phi} = (p_m - w_p) + (q_m - w_q)\sin\phi\tan\theta + (r_m - w_r)\cos\phi\tan\theta \tag{4}$$

$$\dot{\theta} = (q_m - w_q)\cos\phi - (r_m - w_r)\sin\phi \tag{5}$$

$$\dot{\psi} = (q_m - w_q)\frac{\sin\phi}{\cos\theta} + (r_m - w_r)\frac{\cos\phi}{\cos\theta} \tag{6}$$

Define:

$$x = [V\ \alpha\ \beta\ \phi\ \theta\ \psi]^T,\ w = [w_{Ax}\ w_{Ay}\ w_{Az}\ w_p\ w_q\ w_r]^T \tag{7}$$

$$u_m = [A_{xm}\ A_{ym}\ A_{zm}\ p_m\ q_m\ r_m]^T = [A_x\ A_y\ A_z\ p\ q\ r]^T + w \tag{8}$$

where $x \in \mathbb{R}^n$ is the state vector, $u_m \in \mathbb{R}^l$ is the measured input vector. V is the true airspeed, α is the angle of attack, β is the angle of sideslip. ϕ, θ and ψ are the roll angle, pitch angle and yaw angle, respectively. The input vector, denoted as u_m, is the measurement from Inertial Measurement Unit (IMU) sensors. The subscript "m" indicates a measured quantity. A_x, A_y, A_z are the specific forces, p, q, and r are the roll rate, pitch rate and yaw rate, respectively. w is the noise in the IMU sensor with covariance matrix defined as:

$$E[w(t)w^T(t_\tau)] = Q\delta(t - \tau). \tag{9}$$

The above process model can be rewritten into the following vector form:

$$\dot{x}(t) = \bar{f}(x(t), u_m(t), t) + G(x(t))w(t) \tag{10}$$

Further define the following:

$$y_m = [V_m\ \alpha_m\ \beta_m\ \phi_m\ \theta_m\ \psi_m]^T,\ v = [v_V\ v_\alpha\ v_\beta\ v_\phi\ v_\theta\ v_\psi]^T,\ f = [f_V\ f_\alpha\ f_\beta\ f_\phi\ f_\theta\ f_\psi]^T \tag{11}$$

where $y_m \in \mathbb{R}^m$ is the measurement vector, $f \in \mathbb{R}^p$ is the fault vector. $[f_V \ f_\alpha \ f_\beta]^T$ denotes the faults in the ADSs and $[f_\phi \ f_\theta \ f_\psi]^T$ denotes the faults in the AHRS. v is the output noise vector with

$$E[v(t_i)v^T(t_j)] = R\delta(t_i - t_j). \tag{12}$$

The measurement model including the ADS and AHRS faults is:

$$y_m(t) = h(x(t)) + F(t)f(t) + v(t) \tag{13}$$

$$= H(t)x(t) + F(t)f(t) + v(t), \quad t = t_i, \ i = 1, 2, ... \tag{14}$$

where $H = F = I_{6\times 6}$.

B. Design of the sensor fault reconstruction system

To design the ATS-UKF [13], first the condition for fault reconstruction is checked. In this study, $m = 6$, $p = 6$ and rank $F_k = 6$. According to [13, 34], the condition is satisfied and an ATS-UKF can be designed. The ATS-UKF, proposed in [13], is generalized into the following three steps to estimate the states and faults. In [13], only ADS faults are considered while in this paper, both ADS and AHRS faults are considered.

Step1 Time update

$$\mathcal{X}_{i,k|k-1} = \mathcal{X}_{i,k-1} + \int_{k-1}^{k} \bar{f}(\mathcal{X}_{i,k-1}, u(t), t)dt \tag{15}$$

$$\hat{x}_{k|k-1} = \sum_{i=0}^{2n} w_i^{(m)} \mathcal{X}_{i,k|k-1} \tag{16}$$

$$P_{k|k-1} = \sum_{i=0}^{2n} w_i^{(c)} [\mathcal{X}_{i,k|k-1} - \hat{x}_{k|k-1}][\mathcal{X}_{i,k|k-1} - \hat{x}_{k|k-1}]^T + Q_d \tag{17}$$

$$\mathcal{Y}_{i,k|k-1} = h(\mathcal{X}_{i,k|k-1}) \tag{18}$$

$$\hat{y}_k = \sum_{i=0}^{2n} w_i^{(m)} \mathcal{Y}_{i,k|k-1} \tag{19}$$

$$P_{xy,k} = \sum_{i=0}^{2n} w_i^{(c)} [\mathcal{X}_{i,k|k-1} - \hat{x}_{k|k-1}][\mathcal{Y}_{i,k|k-1} - \hat{y}_k]^T \tag{20}$$

$$P_{yy,k} = \sum_{i=0}^{2n} w_i^{(c)} [\mathcal{Y}_{i,k|k-1} - \hat{y}_k][\mathcal{Y}_{i,k|k-1} - \hat{y}_k]^T + R \tag{21}$$

where $\mathcal{X}_{i,k-1}$ is the sigma point vector which is generated using the state estimation and covariance of estimation error at time step $k-1$ denoted as $\hat{x}_{k-1|k-1}$ and $P_{k-1|k-1}$ respectively [35]. $w_i^{(m)}$ and $w_i^{(c)}$ are the weights which can be found in [13, 36]. $\hat{y}_k$ is the estimate of the measurements. $P_{xy,k}$ and $P_{yy,k}$ are covariance matrices. Q_d is approximated by $G(\hat{x}_{k|k-1})QG(\hat{x}_{k|k-1})^T\Delta t$ and Δt is the time step.

Step2 Detection, isolation and estimation of the faults

Define C_k as follows:

$$C_k := \frac{1}{N}\sum_{j=k-N+1}^{k}\boldsymbol{\gamma}_j\boldsymbol{\gamma}_j^T \tag{22}$$

where $\boldsymbol{\gamma}_j = (y_j - \hat{y}_j)$, denotes the innovation at time step j. In this paper, $N = 10$.

Let $C_{ii,k}$, $i = 1, 2, ..., m$ denote the ith diagonal elements of C_k at time step k. The fault detection and isolation is performed through the following:

$$\text{If } C_{ii,k} > T_i,\ F_{A_i} = 1.\ \text{otherwise } F_{A_i} = 0,\ i = 1, 2, ..., m.$$

where $F_A = [F_{A_V}\ F_{A_\alpha}\ F_{A_\beta}\ F_{A_\phi}\ F_{A_\theta}\ F_{A_\psi}]^T$ is the vector of binary alarm indicators. T_i is the vector of thresholds which are designed to detect the faults in the ADS and AHRS respectively. These thresholds are designed based on fault-free cases.

To cope with initial condition errors, we need to calculate the change of the innovation covariance $\Delta C_{ii,k}$ as follow[13]:

$$\Delta C_{ii,k} := C_{ii,k} - C_{ii,k-1}, \quad i = 1, 2, ..., m. \tag{23}$$

When the following inequality holds, the initial measurement update can be regarded as sufficient. The inequality is

$$\Delta C_{ii,k} < \eta_i, \quad i = 1, 2, ..., m. \tag{24}$$

where η_i, $i = 1, 2, ..., m$ are pre-defined constants which can be tuned to stop the initial measurement update. It should be noted that this initial measurement update is only performed in the first few time steps denoted by k^*. In this paper, $k^* = 20$.

If either of the following two conditions is satisfied:

(a) There are no faults detected (i.e., $\|F_A\| = 0$)

(b) $k < k^*$ and $\Delta C_{ii,k} > \eta_i$ for all $i = 1, 2, ..., m$

the estimates of the fault and its error covariance matrix are:

$$\hat{f}_k = 0,\ P_k^f = 0 \tag{25}$$

If neither of conditions (a) and (b) is satisfied, the estimates of the fault and its error covariance matrix are calculated as follows:

$$N_k = (F_k^T P_{yy,k}^{-1} F_k)^{-1} F_k^T P_{yy,k}^{-1} \tag{26}$$

$$\hat{f}_k = N_k \gamma_k,\ P_k^f = (F_k^T P_{yy,k}^{-1} F_k)^{-1} \tag{27}$$

where γ_k is the innovation at time step k, $\hat{f}_k$ is the estimation of f_k and P_k^f is its error covariance matrix. N_k is the gain matrix which can achieve an unbiased estimation of f_k.

Step3 Measurement update

$$K_k = P_{xy,k} P_{yy,k}^{-1} \tag{28}$$

$$\hat{x}_{k|k} = \hat{x}_{k|k-1} + K_k(y_k - \hat{y}_k - F_k \hat{f}_k) \tag{29}$$

$$P_{k|k} = P_{k|k-1} - K_k(P_{yy,k} - F_k P_k^f F_k^T) K_k^T \tag{30}$$

By substituting the functions $\bar{f}$ and h given in Eqs. (10) and (13) into Eqs. (15) and (18) respectively, the fault estimation and state estimation can be achieved which are given in Eqs. (27) (or (25)) and (29) respectively. The state and fault estimation results are used by the controller which is designed in the following section.

III. Reconfigurable Control: Incremental Backstepping

This section will introduce the reconfigurable control approach for the actuator FTC. First, in section III A, the dynamics of the aircraft attitude and angular rates are presented. Then, the design of the IBS controller for actuator FTC is presented in section III B.

A. Aircraft attitude and angular rate dynamics

In this section, the attitude dynamics and angular rate dynamics of the aircraft are presented, which is the model used for designing the IBS controller. The kinematics of the Euler angles are:

$$\begin{bmatrix} \dot{\phi} \\ \dot{\theta} \end{bmatrix} = \begin{bmatrix} 1 & \sin\phi\tan\theta & \cos\phi\tan\theta \\ 0 & \cos\phi & -\sin\phi \end{bmatrix} \omega \tag{31}$$

with $\omega = [p\ q\ r]^T$ the rotational rates of the aircraft in the body reference frame. Furthermore, the sideslip angle β has to be kept at zero. The dynamics of the sideslip angle are given in Eq. (3).

Eqs. (31) and (3) can be rewritten into:

$$\dot{x}_1 = f_1(x_1) + g_1(x_1)x_2 \tag{32}$$

where

$$x_1 = [\phi, \theta, \beta]^T, x_2 = \omega,$$

$$f_1 = \begin{bmatrix} 0 \\ 0 \\ \frac{1}{V}\big[-(A_x - g\sin\theta)\cos\alpha\sin\beta + (A_y + g\sin\phi\cos\theta)\cos\beta - (A_z + g\cos\phi\cos\theta)\sin\alpha\sin\beta\big] \end{bmatrix}$$

$$g_1 = \begin{bmatrix} 1 & \sin\phi\tan\theta & \cos\phi\tan\theta \\ 0 & \cos\phi & -\sin\phi \\ \sin\alpha & 0 & -\cos\alpha \end{bmatrix} \tag{33}$$

The angular rate dynamics of the aircraft are:

$$\dot{\omega} = J^{-1}(M - \omega \times J\omega) \tag{34}$$

where J is the inertia tensor. M are the moments acting on the aircraft which can be described as:

$$M = M_a + M_u = M_a + C_{M_u}u \tag{35}$$

where M_a are the moments except for the moments generated by the control surface deflections. M_u are the moments generated by the control surface deflections. C_{M_u} are the coefficients related

to M_u, which are denoted as

$$M_a = \bar{q}SC_1 \begin{bmatrix} C_l(\beta, p, r, M_a) \\ C_m(\alpha, \dot{\alpha}, q, M_a) \\ C_n(\beta, p, r, M_a) \end{bmatrix}, C_{M_u} = \bar{q}SC_1 \begin{bmatrix} C_{l_{\delta a}} & 0 & C_{l_{\delta r}} \\ 0 & C_{m_{\delta e}} & 0 \\ C_{n_{\delta a}} & 0 & C_{n_{\delta r}} \end{bmatrix}, C_1 = \text{diag}(b, \bar{c}, b) \tag{36}$$

where $\bar{q}$ is the dynamic pressure, M_a is the Mach number, S is the wing area, b the wing span and $\bar{c}$ is the mean aerodynamic chord. The control surface deflections are $u = [\delta_a, \delta_e, \delta_r]^T$, which are also the input to the system.

Eq. (34) can be rewritten into the following affine-in-control form:

$$\dot{x}_2 = f_2(x_1, x_2) + g_2 u \tag{37}$$

where $f_2 = J^{-1}(M_a - \omega \times J\omega)$, $g_2 = J^{-1}C_{M_u}$.

B. Incremental Backstepping Controller Design

In order to design the IBS controller, we need to rewrite Eq. (37) into an incremental form. Denote the actuator deflections in the previous time step as u_0 and the incremental deflections in the current step as Δu, then the actuator deflections in the current step are:

$$u = u_0 + \Delta u \tag{38}$$

where $u_0 = [\delta_{a0}, \delta_{e0}, \delta_{r0}]^T$ and $\Delta u = [\Delta\delta_a, \Delta\delta_e, \Delta\delta_r]^T$. u_0 can be obtained using the actuator model [28]. According to [37], Eq. (37) can be rewritten into the following:

$$\dot{x}_2 = \dot{x}_{2,0} + g_2 \Delta u \tag{39}$$

where $\dot{x}_{2,0}$, the derivative of the angular rates in the previous time step, is defined as:

$$\dot{x}_{2,0} := f_2(x_{10}, x_{20}) + g_2 u_0 \tag{40}$$

$\dot{x}_{2,0}$ can be computed by passing ω_m ($[p_m, q_m, r_m]^T$) through the following filter:

$$\frac{s\omega_n^2}{s^2 + 2\zeta_n\omega_n s + \omega_n^2} \tag{41}$$

with $\zeta_n = 0.8$, $\omega_n = 25$ rad/s chosen by trial and error to reduce the influence of noise [37].

Now the complete model used for the controller design can be given as follows:

$$\begin{cases} \dot{x}_1 = f_1(x_1) + g_1(x_1)x_2 & (42) \\ \dot{x}_2 = \dot{x}_{2,0} + g_2\Delta u & (43) \end{cases}$$

Now the design of the controller based on the model Eqs. (42) and (43) can be presented. The control task is to steer x_1 towards a given reference $y_r = [\phi^{ref}, \theta^{ref}, \beta^{ref}]^T$ with bounded and known derivatives ($\dot{y}_r$, $\ddot{y}_r$, ...). Define the following tracking errors:

$$z_1 = x_1 - y_r \tag{44}$$

$$z_2 = x_2 - \alpha_1 \tag{45}$$

where α_1 is the virtual control for the state x_2. The derivatives of Eqs. (44) and (45) are:

$$\dot{z}_1 = \dot{x}_1 - \dot{y}_r \tag{46}$$

$$\dot{z}_2 = \dot{x}_2 - \dot{\alpha}_1 \tag{47}$$

Substituting Eqs. (42) and (43) into Eqs.(46) and (47), it follows that

$$\dot{z}_1 = f_1(x_1) + g_1(x_1)x_2 - \dot{y}_r \tag{48}$$

$$\dot{z}_2 = \dot{x}_{2,0} + g_2\Delta u - \dot{\alpha}_1 \tag{49}$$

Define $\bar{z}_1 = z_1 - \chi_1$ and $\bar{z}_2 = z_2 - \chi_2$. By using the control Lyapunov function $V = \frac{1}{2}\bar{z}_1^T\bar{z}_1 + \frac{1}{2}\bar{z}_2^T\bar{z}_2$, the desired control laws are defined as:

$$\alpha_1 = g_1^{-1}(-c_1 z_1 - f_1(x_1) + \dot{y}_r) \tag{50}$$

$$\Delta u^{des,0} = g_2^{-1}(-g_1(x_1)\bar{z}_1 - c_2 z_2 + \dot{x}_2^{des} - \dot{x}_{2,0}) \tag{51}$$

where c_1 and c_2 are the controller gains. $\dot{x}_2^{des}$ is the filtered derivative of $x_2^{des,0}$ which is defined as:

$$x_2^{des,0} = [p^{des,0}, q^{des,0}, r^{des,0}]^T = \alpha_1 - \chi_2 \tag{52}$$

χ_1 and χ_2 are computed as:

$$\dot{\chi}_1 = -c_1\chi_1 + g_1(x_2^{des} - x_2^{des,0}) \tag{53}$$

$$\dot{\chi}_2 = -c_2\chi_2 + g_2(\Delta u^{des} - \Delta u^{des,0}) \tag{54}$$

Define the following variables:

$$x_2^{des,0} = [p^{des,0}, q^{des,0}, r^{des,0}]^T,\ x_2^{des} = [p^{des}, q^{des}, r^{des}]^T \tag{55}$$

$$\Delta u^{des,0} = [\Delta\delta_a^{des,0}, \Delta\delta_e^{des,0}, \Delta\delta_r^{des,0}]^T,\ \Delta u^{des} = [\Delta\delta_a^{des}, \Delta\delta_e^{des}, \Delta\delta_r^{des}]^T \tag{56}$$

$x_2^{des,0}$ is filtered through second-order command filters [27, 38] to compute x_2^{des} and $\dot{x}_2^{des}$. $\Delta u^{des,0}$ is filtered through second-order command filters to compute Δu^{des}. Take $x_2^{des,0}$ for example, the command filter is as follows [27, 38]:

$$\begin{bmatrix} \dot{q}_1 \\ \dot{q}_2 \end{bmatrix} = \begin{bmatrix} q_2 \\ 2\zeta_c\omega_c\big[S_R(\frac{\omega_c^2}{2\zeta_c\omega_c}[S_P(x_2^{des,0}) - q_1]) - q_2\big] \end{bmatrix} \tag{57}$$

where S_P and S_R are position and rate limit functions [27, 38]: Then $x_2^{des} = q_1$ and $\dot{x}_2^{des} = q_2$.

The final desired control input u^{des} is given by:

$$u^{des} = [\delta_a^{des}, \delta_e^{des}, \delta_r^{des}]^T = u_0 + \Delta u^{des} \tag{58}$$

This concludes the design for the IBS for the feedback system. The IBS approach is robust to the uncertainties in the plant dynamics term since it does not require the information of the plant dynamics. The robustness with respect to the uncertainties in the control effectiveness as well as actuator faults is analyzed in [29].

IV. Fault-Tolerant Control system for dealing with simultaneous sensor and actuator faults

The proposed FTC system for dealing with simultaneous sensor and actuator faults is presented in Fig. 1. As can be seen from the figure, there are two control loops: attitude control loop and rate control loop. The attitude controller follows the commands ϕ^{ref}, θ^{ref} and β^{ref} and is designed based on the BS control law. The attitude control loop generates the reference commands p^{des}, q^{des} and r^{des} for the angular rate control loop. The rate control loop is designed based on the IBS approach and it generates the command for the control surface deflections denoted as δ_a^{des}, δ_e^{des} and δ_r^{des}. The actual control surface deflections are denoted as δ_a, δ_e and δ_r.

The key point of this simultaneous sensor and actuator FTC system is that the sensor FDD makes use of the kinematic model rather than the dynamic model which uses the actuator deflections as the input. In Fig. 1, it is seen that the sensor FDD system does not require any information

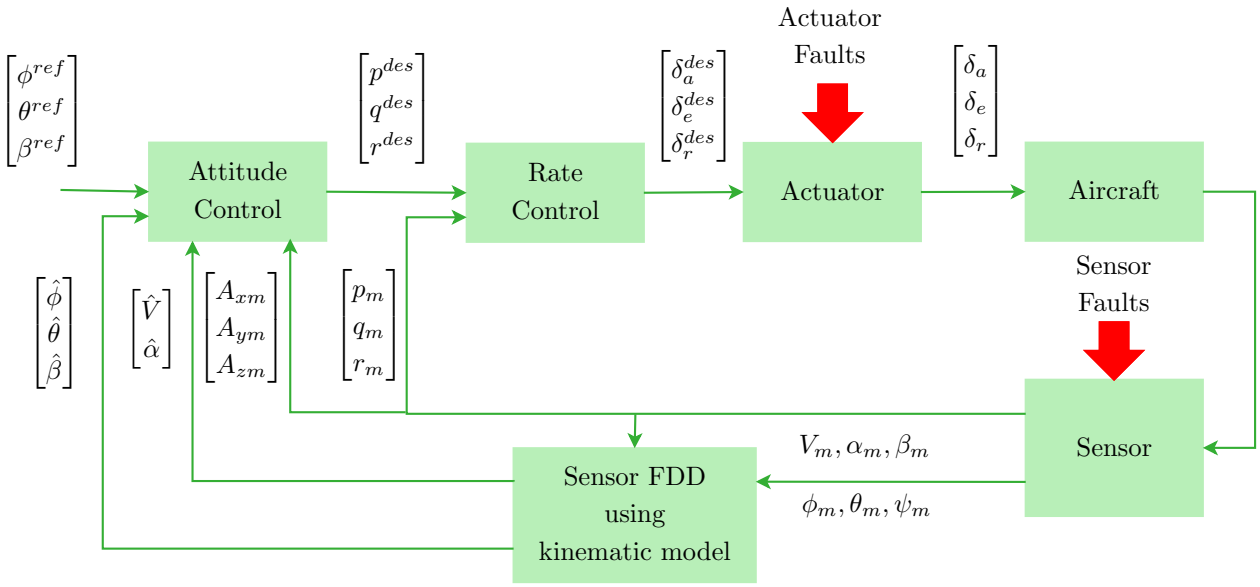

Fig. 1: Block diagram of the FTC system in the presence of sensor and actuator faults

about the actuators such as commanded actuator deflections. In most aircraft sensor FDD system designs, sensor FDD is achieved using the commanded or measured control surface deflections. In some cases, measurements of control surfaces are not available and are derived from the actuator rod positions [39]. Wrong actuator deflections can be obtained when the control surface is disconnected from the actuator rod [39]. Consequently, it can lead to performance degradation of the sensor FDD system.

Reconfigurable controllers can deal with actuator faults. However, it is difficult for these controllers to deal with sensor faults. Therefore, the sensor FDD plays a critical role in this FTC system. The sensor FDD system not only provides unbiased fault estimation ($\hat{f}_V$, $\hat{f}_\alpha$, $\hat{f}_\beta$, and $\hat{f}_\phi$, $\hat{f}_\theta$, $\hat{f}_\psi$) but also unbiased state estimation ($\hat{V}$, $\hat{\alpha}$, $\hat{\beta}$, and $\hat{\phi}$, $\hat{\theta}$, $\hat{\psi}$) such that the performance of the actuator FTC system is not influenced by sensor faults.

V. Simulation examples

In this section, the proposed FTC system against sensor and actuator faults will be validated. In Section V A, the aircraft model and the fault scenarios are presented. The design parameters used in the simulation are presented in Section V B. The performance of the sensor FDD system compared

to that without the sensor FDD system in the presence of sensor faults is shown in Section V C. The performance of the FTC system in the presence of simultaneous sensor and actuator faults is shown in Section V D. Some discussions are presented in Section V E.

A. Aircraft model and fault scenario

The aircraft model used in this paper is the citation model [22]. Due to the page limit, the interested readers can refer to [22] for a more detailed introduction of the actuator. The actuators are modeled as first-order low-pass filters. The control surfaces are left aileron, right aileron, upper rudder, lower rudder and elevator and the deflections are denoted as δ_{al}, δ_{ar}, δ_{ru}, δ_{rl} and δ_e respectively. The desired commands of the ailerons and rudders are as follows:

$$\delta_{al}^{des} = \delta_{ar}^{des} = \delta_a^{des} \tag{59}$$

$$\delta_{ru}^{des} = \delta_{rl}^{des} = \delta_r^{des} \tag{60}$$

This paper considers both sensor faults and actuator faults. The sensor measurements contain noise. The noise covariances of the sensors in the aircraft can be found in [13]. Sensor faults include ADS sensor faults and AHRS faults. All the sensor faults occur simultaneously. The fault scenario of the ADS and AHRS faults is given by dashed lines in Fig. 3. The actuator faults considered in this paper are jamming faults. The specific fault scenario is given in Table 1.

Table 1: Actuator faults

Time interval	Actuator	Fault type	Stuck position	Fault unit
$t > 25$ s	left aileron	Jamming	0.56	[rad]
$t > 75$ s	upper rudder	Jamming	0.2	[rad]

It can be seen that during 25 s $< t <$ 40 s, the left aileron and the ADS and the AHRS fail. During 75 s $< t <$ 80 s, the left aileron, the upper rudder and the ADS and AHRS all fail. Therefore, simultaneous sensor and actuator faults are considered in this paper.

B. FTC system design parameters

In this section, the parameters used for the design of the FTC system is presented. For the sensor FDD, η, which is used in Eq. (24) to terminate the initial measurement update, is chosen as:

$$\eta = [2 \times 10^{-2}, 1 \times 10^{-4}, 1 \times 10^{-5}, 1 \times 10^{-5}, 1 \times 10^{-5}, 1 \times 10^{-5}]^T \tag{61}$$

The threshold T used for fault detection is chosen as:

$$T = [8 \times 10^{-1}, 1 \times 10^{-4}, 1 \times 10^{-4}, 5 \times 10^{-4}, 1 \times 10^{-4}, 2 \times 10^{-4}]^T \tag{62}$$

For the IBS controller, the control gains are chosen as:

$$c_1 = \text{diag}(5, 5, 5), \qquad c_2 = \text{diag}(2, 2, 2) \tag{63}$$

C. Validation of the FTC system in the presence of sensor faults

In this section, the performance of the FTC system in the presence of sensor faults is validated. It is seen from the dashed lines in Fig. 3 that during 20 s $< t <$ 40 s and 60 s $< t <$ 80 s, all the ADS and AHRS fail simultaneously. The sensor FDD system of the FTC system will be used to reconstruct the sensor faults in order to provide unbiased state estimation for the feedback.

For comparison, the IBS controller without the sensor FDD system is also applied. For this controller, the measurements are directly used by the controller. In this case, the state feedback used by the controller is biased due to the sensor faults.

The results of the IBS controller with and without using the sensor FDD system are given in Figs. 2(a) and 2(b) respectively. As can be seen from Fig. 2(a), even in the presence of sensor faults, ϕ, θ and β of the aircraft can still follow the reference commands well. In contrast, when the sensor FDD is not used, ϕ, θ and β of the aircraft can not follow the reference commands when there are sensor faults, as shown in Fig. 2(b). The response of the aircraft is obviously influenced by the wrong sensor measurements. For example, during 20 s $< t <$ 30 s, the reference command for θ is zero. But the aircraft pitches down to -10 deg. This is caused by the θ sensor fault, which is a bias fault. Furthermore, during 60 s $< t <$ 80 s, β reaches 5 deg even when there are no lateral maneuvers. This is not desirable for civil aircraft. The results demonstrate the importance of a sensor FDD system.

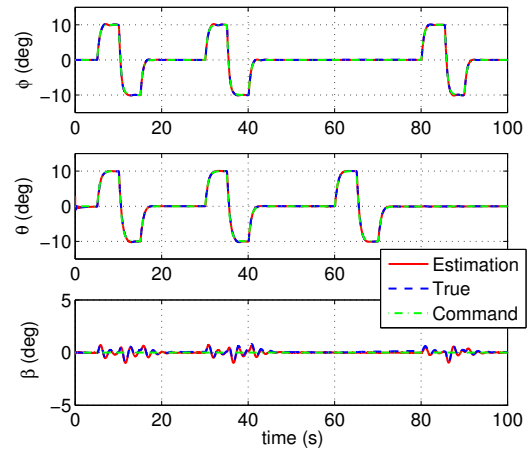

(a) Estimated, true and commanded ϕ, θ and β in the presence of sensor faults, with the sensor FDD system

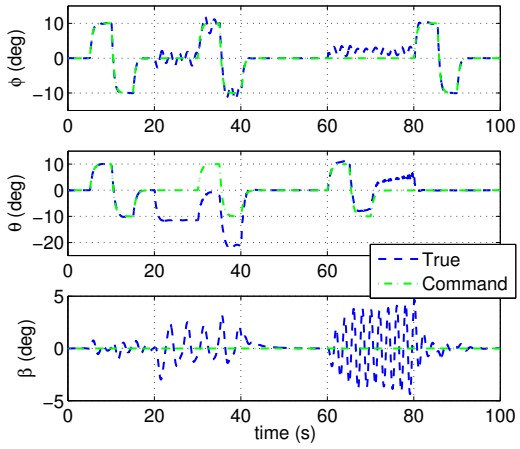

(b) True and commanded ϕ, θ and β in the presence of sensor faults, without the sensor FDD system

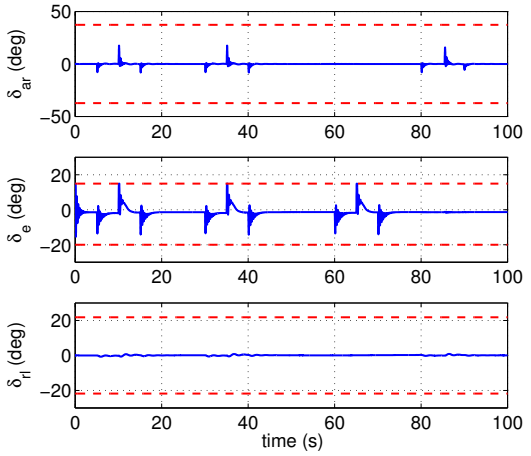

(c) Actuator deflections in the presence of sensor faults with the sensor FDD system. Dashed lines denote the actuator maximum and minimum position limits

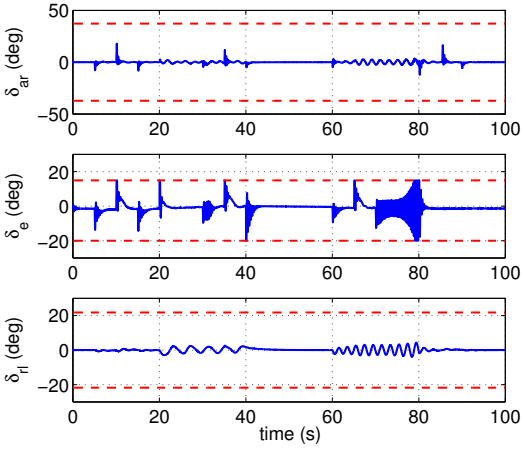

(d) Actuator deflections in the presence of sensor faults without the sensor FDD system. Dashed lines denote the actuator maximum and minimum position limits

Fig. 2: Results of the IBS control with and without the sensor FDD system in the presence of sensor faults

The state estimation performance of the sensor FDD system is shown in Fig. 2(a). It is seen that the solid lines can still follow the dashed lines closely. This demonstrates that the sensor FDD system can provide unbiased state estimation even in the presence of sensor faults.

The actuator control surface deflections δ_{ar}, δ_e and δ_{rl} of the FTC system with the sensor FDD

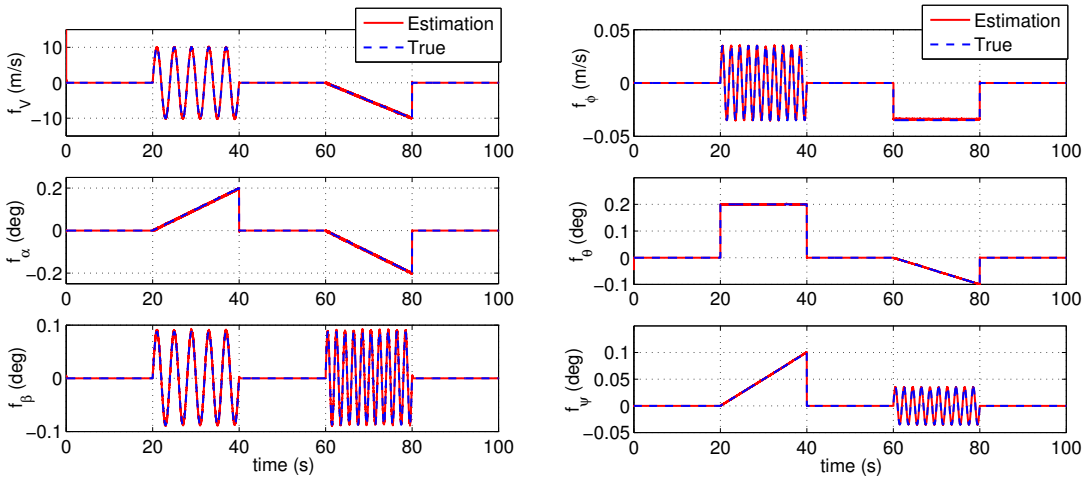

(a) True and estimated f_V, f_α and f_β in the presence of sensor faults

(b) True and estimated f_ϕ, f_θ and f_ψ in the presence of sensor faults

Fig. 3: Fault reconstruction of the sensor FDD system in the presence of sensor faults

system are given in Fig. 2(c). It is seen that all the control surface deflections are within the actuator position limits. The control surface deflections δ_{ar}, δ_e and δ_{rl} of the FTC system without using the sensor FDD system is shown in Fig. 2(d). As can be seen from the figure, the control surfaces oscillate in the presence of sensor faults. During 70 s $< t <$ 80 s, the elevator oscillates frequently, which can even damage the elevator itself.

For the FTC system with sensor FDD, sensor FTC is achieved. The fault reconstruction results using the sensor FDD system are given in Figs. 3(a) and 3(b). It is seen from the figure, although the fault types are different, all faults are reconstructed in an unbiased sense. The oscillatory frequency of the oscillatory faults are also different. This demonstrates the performance of the sensor FDD system which makes use of the ATS-UKF.

D. Validation of the FTC system in the presence of simultaneous sensor and actuator faults

In this section, the performance of the FTC system in the presence of simultaneous sensor and actuator faults is validated. The actuator faults are given in Table 1. The sensor faults are coped with by the sensor FDD system. The actuator faults are dealt with by the IBS approach. The results of the FTC system are given in Fig. 4.

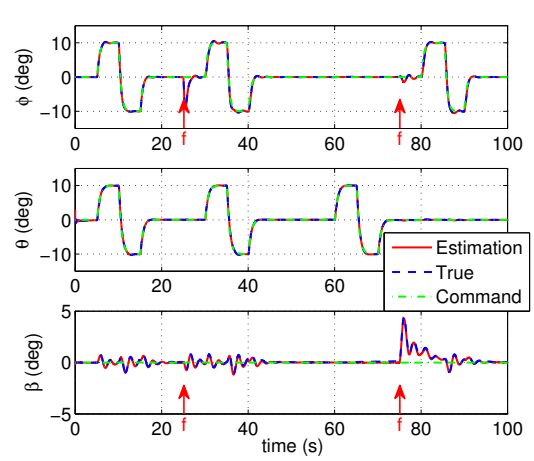

(a) Estimated, true and commanded ϕ, θ and β in the presence of simultaneous sensor and actuator faults. The arrows denote the occurrence of the faults.

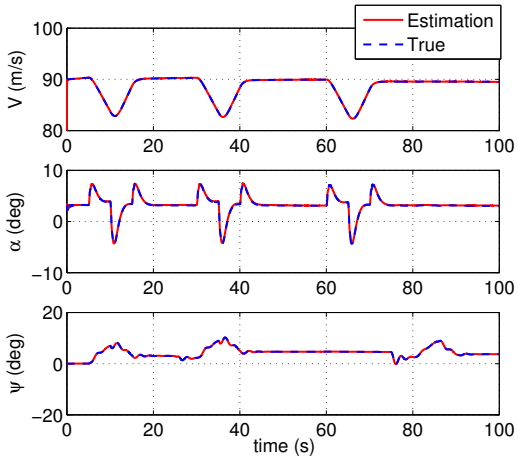

(b) Estimated and true V, α and ψ in the presence of simultaneous sensor and actuator faults

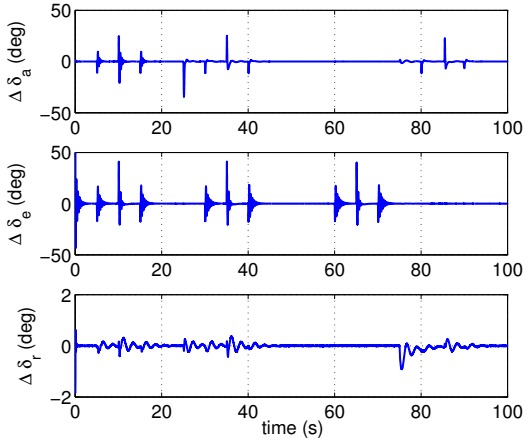

(c) Incremental actuator deflections in the presence of simultaneous sensor and actuator faults

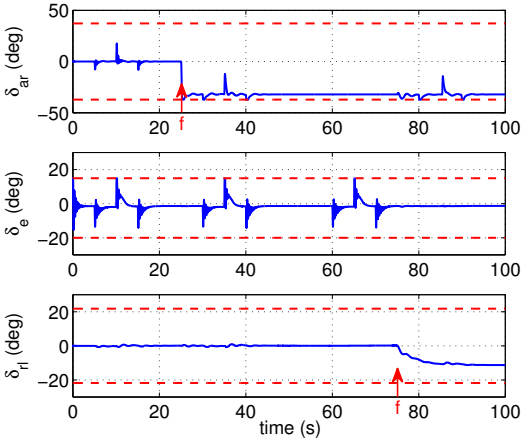

(d) Actuator deflections in the presence of simultaneous sensor and actuator faults. Dashed lines denote position limits. Arrows denote the occurrence of the faults.

Fig. 4: Results of the FTC system in the presence of simultaneous sensor and actuator faults

The response of ϕ, θ and β of the aircraft using the FTC system is shown in Fig. 4(a). As can be seen from the figure, when the actuators are stuck, ϕ and β will be influenced and deviate from zero. However, ϕ and β are controlled back to zero thanks to the IBS controller.

The state estimation performance remains satisfactory. Estimated and true ϕ, θ and β are shown in Fig. 4(a) while those of V, α and ψ are shown in Fig. 4(b). It can be seen that the state

estimation is unbiased despite the sensor and actuator faults.

The incremental control surface deflections generated by the IBS controller are shown in Fig. 4(c). The actual control surface deflections δ_{ar}, δ_e and δ_{rl} are shown in Fig. 4(d). It is seen from the figure that the control surface deflections change after the occurrence of the faults. Take the ailerons for example, after the left aileron is stuck at a positive position at $t = 25$ s, the IBS controller takes effect. The desired command δ_a^{des} generated by the IBS decreases immediately. Then the right aileron deflects to a negative position. By doing this, the moments generated by the stuck left aileron is counteracted by the right aileron which deflects to a negative position.

It is also obvious that the remaining control authority will decrease due to the stuck aileron. Since the left aileron is stuck at a positive position, it generates a negative rolling moment all the time. Therefore, the control authority of rolling to the right is decreased. Therefore, extreme maneuvers should be performed with caution after the actuator faults.

The fault reconstruction using the sensor FDD system is still satisfactory even in the presence of simultaneous sensor and actuator faults. They are the same as those in Figs. 3(a) and 3(b). Therefore, they are not shown again.

E. Discussion

Through the validations in the previous sections, the following conclusions can be made:

1. The sensor FDD system is critical to maintain the performance in the presence of sensor faults. In Section V C, the reconfigurable controller (IBS) has no ability to recover the control in the presence of sensor faults if the sensor FDD is not included. This is expected since the controller relies on the measurements to calculate the error between the reference command and the controlled states. The control objective is to minimize the tracking errors such as those in Eq. (44). Let z_θ denote the tracking error of θ and assume the wrong measurement is directly used by the controller, then

$$z_\theta = \theta_m - \theta^{ref} = \theta + f_\theta + v_\theta - \theta^{ref} \tag{64}$$

If z_θ is minimized to zero by the controller, it can be readily inferred that the true state θ deviates from the command θ^{ref} by $f_\theta + v_\theta$.

2. Simultaneous sensor and actuator FTC can be achieved by decoupling the sensor FTC from the actuator information. Through the validation in Section V D, simultaneous sensor and actuator FTC is achieved by the sensor FDD system and the reconfigurable controller. Since the sensor FDD system does not require the actuator information, it can perform state and fault estimation without being influenced by the actuator faults. The sensor FDD system provides unbiased state and fault estimation such that the reconfigurable controller can perform the reconfiguration without being influenced by sensor faults.

3. Control authority could be reduced after the actuator faults depending on the actuator redundancy. A control allocation technique can be useful for aircraft with actuator redundancy to perform FTC in the presence of actuator faults.

VI. Conclusions

This paper proposes an aircraft Fault-Tolerant Control (FTC) system, which can maintain controlled flight in the presence of simultaneous sensor and actuator faults. The proposed system consists of a sensor Fault Detection and Diagnosis (FDD) system and a reconfigurable controller. The sensor FDD system makes use of the aircraft kinematic model and does not require any information about the actuator deflections. The Adaptive Three-Step Unscented Kalman Filter (ATS-UKF) is used to reconstruct the state and fault in an unbiased sense. The state estimation is used by the controller to achieve sensor FTC. The actuator faults are dealt with by the reconfigurable controller which is the Incremental Backstepping (IBS) in this paper.

The proposed FTC system is validated by simulation examples. The simulated aircraft contains Air Data Sensors (ADS) and Aircraft Heading and Reference System (AHRS) faults as well as stuck actuator faults. The simulation results demonstrate that the proposed FTC system is able to deal with sensor faults as well as actuator faults and maintain the controlled flight.

The simulation results show that sensor and actuator FTC can be achieved simultaneously using model-based analytical redundancy. This FTC system has a potential to be applied to the aircraft to enhance the safety of the aircraft. For future work, the stability of the whole FTC system is worth investigating.

References

1. Lombaerts T, Chu Q, Mulder J, Joosten D. Modular flight control reconfiguration design and simulation. *Control Engineering Practice* 2011;19(6):540–54. doi:10.1016/j.conengprac.2010.12.008.
2. ICAO . Safety Report. Tech. Rep.; International Civil Aviation Organization; 2015.
3. Smaili MH, Breeman J, Lombaerts T, Joosten DA. A Simulation Benchmark for Integrated Fault Tolerant Flight Control Evaluation. In: *AIAA Modeling and Simulation Technologies Conference and Exhibit*. Keystone, Colorado; 2006:1–23.
4. Uncontrolled Descent and Collision with Terrain, United Airlines Flight 585, Boeing 737-200, N999UA, 4 Miles South of Colorado Springs Municipal Airport. Tech. Rep.; National transportation safety board; 2001.
5. Lombaerts T. Fault Tolerant Flight Control- A Physical Model Approach. Ph.D. thesis; Delft University of Technology; 2010.
6. BEA . Final report on the accident on 1st June 2009 to the Airbus A330-203 registered F-GZCP operated by air france flight AF 447 Rio de Janeiro Paris. Tech. Rep. June 2009; Bureau d'Enquêtes et d'Analyses pour la sécurité de l'aviation civile; 2012.
7. ATSB . Atsb transport safety report: In-flight upset 154 km west of Learmonth, WA 7 October 2008 VH-QPA Airbus A330-303. Tech. Rep. October; Australian Transport Safety Bureau; 2008.
8. Patton RJ. Fault-tolerant Control Systems: The 1997 Situation. In: *Proc. of IFAC Symp. on Fault Detection, Supervision and Safety for Technical Processes*. 1997:1033–54.
9. Zolghadri A. Advanced model-based fdir techniques for aerospace systems: Today challenges and opportunities. *Progress in Aerospace Sciences* 2012;53:18–29. doi:10.1016/j.paerosci.2012.02.004.
10. Marzat J, Piet-Lahanier H, Damongeot F, Walter E. Model-based fault diagnosis for aerospace systems: a survey. *Proceedings of the Institution of Mechanical Engineers, Part G: Journal of Aerospace Engineering* 2012;226(10):1329–60. doi:10.1177/0954410011421717.
11. Freeman P, Seiler P, Balas GJ. Air data system fault modeling and detection. *Control Engineering Practice* 2013;21(10):1290–301. doi:10.1016/j.conengprac.2013.05.007.
12. Lu P, Van Eykeren L, van Kampen E, Chu Q. Selective-Reinitialisation Multiple Model Adaptive Estimation for Fault Detection and Diagnosis. *Journal of Guidance, Control, and Dynamics* 2015;38(8):1409–25. doi:10.2514/6.2014-0965.
13. Lu P, Van Eykeren L, van Kampen E, de Visser CC, Chu Q. Adaptive Three-Step Kalman Filter for Air Data Sensor Fault Detection and Diagnosis. *Journal of Guidance, Control, and Dynamics* 2016;39(3):590–604. doi:10.2514/1.G001313.

14. Alwi H, Chen L, Edwards C. Reconstruction of simultaneous actuator and sensor faults for the RECONFIGURE benchmark using a sliding mode observer. In: *The International Federation of Automatic Control World Congress*. 2; Cape Town, South Africa; 2014:3497–502.

15. Varga A, Ossmann D. LPV model-based robust diagnosis of flight actuator faults. *Control Engineering Practice* 2013;31:135–47. doi:10.1016/j.conengprac.2013.11.004.

16. Van Eykeren L, Chu Q. Sensor fault detection and isolation for aircraft control systems by kinematic relations. *Control Engineering Practice* 2014;31:200–10. doi:10.1016/j.conengprac.2014.02.017.

17. Lu P, Van Eykeren L, van Kampen E, de Visser CC, Chu Q. Double-model adaptive fault detection and diagnosis applied to real flight data. *Control Engineering Practice* 2015;36:39–57. doi:10.1016/j.conengprac.2014.12.007.

18. Lu P, van Kampen E, de Visser C, Chu QP. Nonlinear Aircraft Sensor Fault Reconstruction in the Presence of Disturbances Validated by Real Flight Data. *Control Engineering Practice* 2016;49:112–28. doi:10.1016/j.conengprac.2016.01.012.

19. Zhang Y, Jiang J. Bibliographical review on reconfigurable fault-tolerant control systems. *Annual reviews in control* 2008;(32):229–52. doi:10.1016/j.arcontrol.2008.03.008.

20. Yu X, Liu Z, Zhang Y. Fault-Tolerant Flight Control with Finite-Time Adaptation under Actuator Stuck Failures. *IEEE Transactions on Control Systems Technology* 2016;available online. doi:10.1109/TCST.2016.2603072.

21. Yu X, Liu Z, Zhang Y. Fault-Tolerant Flight Control Design with Explicit Consideration of Reconfiguration Transients. *Journal of Guidance, Control, and Dynamics* 2016;39(3):556–63. doi:10.2514/1.G001414.

22. Lu P, van Kampen E, de Visser C, Chu QP. Aircraft Fault-Tolerant Trajectory Control Using Incremental Nonlinear Dynamic Inversion. *Control Engineering Practice* 2016;57:126–41. doi:10.1016/j.conengprac.2016.01.012.

23. Kale MM, Chipperfield AJ. Stabilized MPC formulations for robust reconfigurable flight control. *Control Engineering Practice* 2005;13:771–88. doi:10.1016/j.conengprac.2004.09.001.

24. Utkin VI. Sliding Modes in Control and Optimization. Springer-Verlag Berlin Heidelberg; 1992.

25. Cieslak J, Henry D, Zolghadri A, Goupil P. Development of an Active Fault-Tolerant Flight Control Strategy. *Journal of Guidance, Control, and Dynamics* 2008;31(1):135–47. doi:10.2514/1.30551.

26. Krstic M, Kanellakopoulos I, Kokotovic P. Nonlinear and Adaptive Control Design. John Wiley & Sons, Inc.; 1995.

27. Farrell JA, Polycarpou M, Sharma M, Dong W. Command Filtering Backstepping. *IEEE Transactions*

on Automatic Control 2009;54(6):1391–5. doi:10.1109/TAC.2009.2015562.

28. Acquatella P, van Kampen E, Chu Q. Incremental Backstepping for Robust Nonlinear Flight Control. In: *Proceedings of the EuroGNC 2013, 2nd CEAS Special Conference on Guidance, Navigation & Control*. 2013:1444–63.
29. Lu P, van Kampen E, Chu Q. Robustness and Tuning of Incremental Backstepping. In: *AIAA Guidance, Navigation and Control Conference*. AIAA 2015-1762; Kissimmee, Florida; 2015:1–15.
30. Chen RH, Speyer JL. Sensor and Actuator Fault Reconstruction. *Journal of Guidance, Control, and Dynamics* 2004;27(2):186–96. doi:10.2514/1.9163.
31. Yu X, Jiang J. A survey of fault-tolerant controllers based on safety-related issues. *Annual reviews in control* 2015;(39):46–57. doi:10.1016/j.arcontrol.2015.03.004.
32. Zhang Y, Li X. Detection and diagnosis of sensor and actuator failures using IMM estimator. *IEEE Transactions on Aerospace and Electronic Systems* 1998;34(4):1293–313. doi:10.1109/7.722715.
33. Marzat J, Piet-Lahanier H, Damongeot F, Walter E. Control-based fault detection and isolation for autonomous aircraft. *Proceedings of the Institution of Mechanical Engineers, Part G: Journal of Aerospace Engineering* 2011;226(5):510–31. doi:10.1177/0954410011413834.
34. Gillijns S, De Moor B. Unbiased minimum-variance input and state estimation for linear discrete-time systems with direct feedthrough. *Automatica* 2007;43(5):111–6.
35. Julier SJ, Uhlmann JK. Unscented Filtering and Nonlinear Estimation. In: *Proceedings of the IEEE*; vol. 92. 2004:401–22. doi:10.1109/JPROC.2003.823141.
36. Van Der Merwe R, Wan EA. The Square-root Unscented Kalman Filter for State and Parameter-estimation. In: *IEEE International Conference on Acoustics, Speech, and Signal Processing*. 2001:3461–4.
37. Bacon BJ, Ostroff AJ, Joshi SM. Reconfigurable NDI Controller Using Inertial Sensor Failure Detection & Isolation. *IEEE Transactions on Aerospace and Electronic Systems* 2001;37(4):1373–83.
38. Sonneveldt L, Chu Q, Mulder JA. Nonlinear Flight Control Design Using Constrained Adaptive Backstepping. *Journal of Guidance, Control, and Dynamics* 2007;30(2). doi:10.2514/1.25834.
39. Goupil P. Oscillatory failure case detection in the A380 electrical flight control system by analytical redundancy. *Control Engineering Practice* 2010;18(9):1110–9. doi:10.1016/j.conengprac.2009.04.003.